

# CELLULAR GLASS FROM POST-CONSUMER DRINKING GLASS NON-CONVENTIONALLY PREPARED WITH SILICON NITRIDE AND MANGANESE DIOXIDE AS PORE-FORMING AGENTS

Lucian Paunescu<sup>1</sup>, Sorin Mircea Axinte<sup>2,3</sup> and Alexandru Fiti<sup>4</sup>

<sup>1</sup> Cosfel Actual SRL Bucharest, Romania, [lucianpaunescu16@gmail.com](mailto:lucianpaunescu16@gmail.com)

<sup>2</sup> Daily Sourcing & Research SRL, Bucharest, Romania,  
[sorinaxinte@yahoo.com](mailto:sorinaxinte@yahoo.com)

<sup>3</sup> University "Politehnica" of Bucharest, Department of Applied Chemistry and Materials Science Bucharest, Romania,  
[sorinaxinte@yahoo.com](mailto:sorinaxinte@yahoo.com)

<sup>4</sup> Cosfel Actual SRL Bucharest, Romania,  
[alexandru.fiti@gmail.com](mailto:alexandru.fiti@gmail.com)

**ABSTRACT:** Cellular glass non-conventionally prepared from post-consumer drinking glass was made, silicon nitride ( $\text{Si}_3\text{N}_4$ ) and manganese dioxide ( $\text{MnO}_2$ ) contributing to form the porous structure. The correlation between the physical-morphological properties (low denseness, high porousness, structural homogeneousness) of the expanded material and its strength features (high compression resistance) played an essential role. An optimal weight ratio between the two pore-forming additives was found at the value 1.0. The temperature of the sintering-expanding process was relatively reduced (823 °C) and the warming rate reached very high values (27.7 °C/min) due to the energy efficiency of the own preponderantly direct microwave warming method. The main features of the optimal cellular glass specimen were: denseness of 0.59 g·cm<sup>-3</sup>, heat conduction of 0.097 W·m<sup>-1</sup>·K<sup>-1</sup>, compression resistance of 6.6 MPa, and pore size between 0.1-0.4 mm.

**KEYWORDS:** cellular bottle, wave, preponderantly direct warming, post-consumer drinking bottle, silicon nitride, manganese dioxide.

## 1. INTRODUCTION

In the current global context of industrial manufacturers concern for using the recycled residual bottle as an inexpensive basic material in the manufacturing process of alternative building materials in effective energy terms, different manufacturing variants have been tested in the last two decades. Various pore-forming agents (carbon black, graphite,  $\text{CaCO}_3$ , dolomite,  $\text{Na}_2\text{CO}_3$ , SiC,  $\text{Si}_3\text{N}_4$ , AlN, glycerin, vegetal and animal agents, etc.) were used in the material mixture to release a gas or gaseous compound favouring the creation of gas bubbles and implicitly, the typical porous structure of cellular bottle. Previous works published in the literature have applied manufacturing recipes including numerous variants of expanding agents, additives, and residual bottle types [1-10]. The inclusion of glass on the list of the main waste available in significant amounts in the world is due to their remarkable properties highlighted in the literature [11] such as light weight, low heat conduction, high porousness, resistance to compression stress, fire, water, frost, and different external agent aggression (rodents, insects, bacteria, etc.). In general, consumed container bottle and window bottle from construction decommissioning were the most interesting residual bottle, but also

other glass types (cathode-ray-tube glass, laboratory glass, etc.) were tested.

One of the very efficient pore-providing agents for the preparation of cellular glass is considered silicon nitride ( $\text{Si}_3\text{N}_4$ ). In the paper [5], this expanding agent was used in mixture with flat glass waste and low amounts of manganese dioxide ( $\text{MnO}_2$ ) as an oxygen-supplier supplementary to the existing oxygen in the furnace medium. The mixture expansion process took place in a conventional heating furnace at 800-850 °C) and low holding duration (7-30 min) at the expanding temperature. It was found that when the temperature and the holding duration increase, unwanted effects of the process are produced (the decrease in mechanical strength and the formation of a coarse inhomogeneous microstructure with coalescence cells). According to [5], the mixture pressed in the form of pellets containing glass powder,  $\text{Si}_3\text{N}_4$ , and  $\text{MnO}_2$ , under the conditions of low  $\text{MnO}_2/\text{Si}_3\text{N}_4$  ratio, process temperature below 850 °C, and short holding time, limited the microstructural cell coalescence, and significantly improved the strength of foamed material.

Aspects regarding residual glass foaming by oxidizing SiC,  $\text{Si}_3\text{N}_4$  or AlN as pore-providing agents in association with multivalent metal oxides ( $\text{MnO}_2$ ,  $\text{Fe}_2\text{O}_3$  or  $\text{CeO}_2$ ) were also analyzed in [12]. It was observed that the expanding process achieved

through the associated oxidation/reduction is more intensive and generates more homogeneous microstructures, ensuring a better correlation between physico-morphological, and mechanical properties of foamed products.

As noted in other previous works, glass-expanding processes through conventional heating are still predominant worldwide. Both industrial and small-scale experimental processes are carried out by conventional methods, although the non-conventional technique of heating through electromagnetic waves (microwaves) is faster and more economical.

Several experiments aimed at the production of cellular glass have been performed since 2017 within the societies Daily Sourcing & Research SRL and Cosfel Actual SRL (Romania). The method was based on the own conception preponderantly direct microwave heating and partially indirect heating (through radiation) by placing a protective ceramic screen between the wave flow source and the sample subject to heating. This method was successfully applied by authors of this work for preparing the cellular bottle using residual window bottle as basic material,  $\text{Si}_3\text{N}_4$  and  $\text{MnO}_2$  as pore-forming agents [13]. The amount of  $\text{Si}_3\text{N}_4$  used in this experiment was kept constant in all tested versions (2 wt. %),  $\text{MnO}_2$  having variable values between 2-5.5 wt. %. Therefore, the  $\text{MnO}_2/\text{Si}_3\text{N}_4$  ratio varied between 1-2.75. The results of the specimen characteristics showed that in the case of the minimum ratio, the porousness had the lowest value (72.9 %), the denseness reached the highest level ( $0.57 \text{ g}\cdot\text{cm}^{-3}$ ) as well as the compression resistance (7.8 MPa). The pore size had the lowest values included in the range of 0.10-0.35 mm. Instead, the highest limits of the mentioned ratio (2.10-2.75) corresponding to versions 3 and 4 led to high porousness (82.9-85.6 %), small values of denseness ( $0.36\text{-}0.38 \text{ g}\cdot\text{cm}^{-3}$ ), but the lowest values of compression resistance (3.2-4.9 MPa). Although the compression resistance value is decreasing, the resistance level remains sufficiently high. The use of microwave heating led to high heating rates (19.1-22.7 °C/min), short process durations (35-44 min), and very small specific energy consumption (0.78-0.98 kWh/kg).

The current paper started from the same efficient system of predominantly direct microwave heating designed by authors' team, changing the origin of the recycled residual glass (post-consumer drinking glass, which replaces the flat glass recovered from building demolition used in the reference work [13]).

## 2. METHODS AND MATERIALS

### 2.1 Methods

The adopted procedure was based on the following principles:

- Residual bottle used as basic material has combined post-consumer colourless, green, and amber drinking bottle in roughly equal weight proportions, unlike the clear flat glass used in the reference experiment [13].
- The powder mixture has incorporated  $\text{Si}_3\text{N}_4$  and  $\text{MnO}_2$  as pore-forming agents.
- The mixture heating at relatively low temperatures (below 840 °C), made by microwave radiation, was quickly performed with high heating rates (over 23 °C/min), the holding time at the expanding temperature being negligible (easily achievable considering the very low thermal inertia of microwave heating processes).
- The microwave heating method applied in the experiment was preponderantly direct and partially indirect due to the introduction of a cylindrical SiC and  $\text{Si}_3\text{N}_4$  (80/20 ratio) tube, having excellent microwave susceptibility, positioned between the wave emission waveguide and the pressed mixture for warming. The low tube wall thickness (2.5 mm) is necessary for the preponderant passing of the tube wall and the initiation of direct warming in the core of material [14].

Previous research on the mechanism of the microwave heating process has found that the microwave, which is only an energy carrier, activates its power through direct contact with the material, the power being turned into warm. According to [15, 16], the warming process is started in the central area of the irradiated sample, where the highest hot point is achieved. Heat propagation volumetrically occurs in the entire mass of the sample, from the hot interior to the exterior, the process being fast and effective in terms of energy. By comparison with conventional warming processes, the non-conventional method of microwave warming is completely different, unfolding in the opposite direction. Therefore, advanced thermal protection of the outer surface of material (if it is freely placed) or of the protective crucible (if this solution is adopted) is essential.

Figure 1 shows the microwave experimental equipment, including its construction scheme, designed for the current experiment.

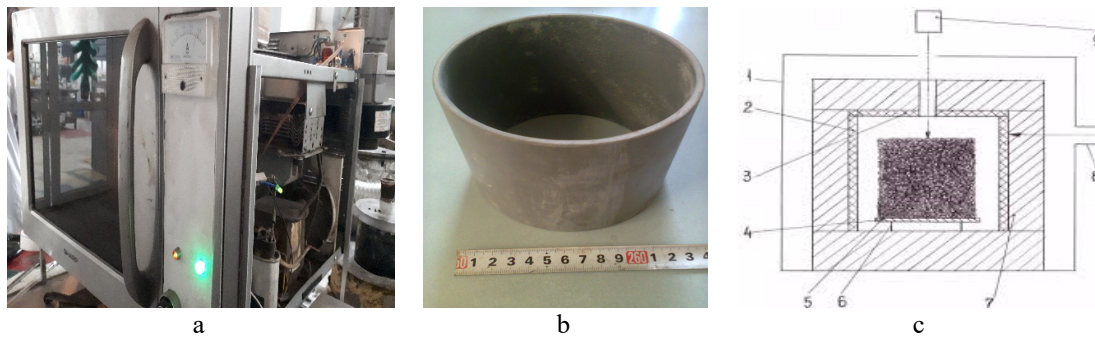
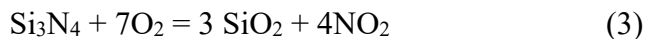
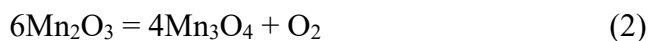
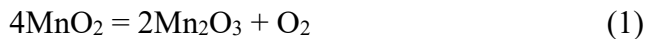


**Figure 1.** Designed equipment for the experiment

a – 800 W-wave furnace; b – cylindrical tube; c – constructive scheme: 1 – adapted furnace; 2 – tube; 3 – lid; 4 – plate; 5 – sample; 6 – support; 7 – heat protection layer; 8 – waveguide; 9 – pyrometer.

In technological terms, the expanding process of bottle powder using the combination of  $\text{Si}_3\text{N}_4$  as a pore-supplying material and  $\text{MnO}_2$  as an oxygen-providing material includes several stages. At  $485^\circ\text{C}$ , the decomposition of  $\text{MnO}_2$  into  $\text{Mn}_2\text{O}_3$  and  $\text{O}_2$  (1) begins, reaching the maximum intensity at  $590^\circ\text{C}$ . The decomposition of  $\text{Mn}_2\text{O}_3$  (2) begins at  $650^\circ\text{C}$ , reaching the highest reaction intensity at  $800^\circ\text{C}$  and releasing  $\text{Mn}_3\text{O}_4$  and  $\text{O}_2$  [17]. The  $\text{Si}_3\text{N}_4$  oxidation (reaction 3) using the previously released oxygen occurs within the limits of  $800\text{-}900^\circ\text{C}$  [18] releasing  $\text{NO}_2$  in the softened bottle mass.



## 2.2 Materials

The component matters materials of the mix were consumed colourless, green, and amber drinking bottle dosed in approximately equal amounts,  $\text{Si}_3\text{N}_4$  commercially procured with a grain size under  $10\ \mu\text{m}$ , and  $\text{MnO}_2$  also purchased from the market with a grain size under  $50\ \mu\text{m}$ .

Residual bottles were selected, washed, crushed, ground, and sieved, the grain sizes being less than  $90\ \mu\text{m}$ . The oxide composition of the three bottle types is presented in Table 1.

**Table 1.** Oxide composition of bottle

Composition	Colourless bottle (wt. %)	Green bottle (wt. %)	Amber bottle (wt. %)
$\text{SiO}_2$	71.8	71.6	71.3
$\text{Al}_2\text{O}_3$	1.9	1.9	2.0
$\text{CaO}$	11.8	11.9	12.1
$\text{Fe}_2\text{O}_3$	0.1	0.1	0.2
$\text{MgO}$	1.1	1.2	1.1

$\text{Na}_2\text{O}$	13.2	13.1	13.0
$\text{K}_2\text{O}$	0.1	0.1	0.1
$\text{Cr}_2\text{O}_3$	0.1	0.1	0.1
$\text{SO}_3$	-	-	0.1

Four recipes of making cellular bottle (R1-R4) were adopted by authors. Weight proportion of components corresponding to these recipes were presented in Table 2.

**Table 2.** Composition of testing recipes

Composition	Recipe (wt. %)			
	R1	R2	R3	R4
Recycled bottle	96.4	96.2	95.6	95.1
$\text{Si}_3\text{N}_4$	1.9	1.9	2.0	2.0
$\text{MnO}_2$	1.7	1.9	2.4	2.9
Water added	13.5	13.5	14.0	14.0
$\text{MnO}_2/\text{Si}_3\text{N}_4$ ratio	0.89	1.00	1.20	1.45

Considering the previous conclusion that the increase of the  $\text{MnO}_2/\text{Si}_3\text{N}_4$  ratio during the manufacture of the cellular bottle from window bottle utilizing  $\text{Si}_3\text{N}_4$  and  $\text{MnO}_2$  [13] disfavours the microstructural homogeneity of the product as well as the level of its mechanical resistance, the dosage of these materials was limited to significantly lower values of  $\text{MnO}_2$ . By default, the  $\text{MnO}_2/\text{Si}_3\text{N}_4$  ratio no longer reached high values, the range being included in the limits of 0.89-1.45.

## 2.3 Methods of investigating the sample features

Denseness and porousness were measured by applying the Archimedes' method according to ASTM D792-20 [19]. The measure of compression resistance was made with TA.XTplus Texture analyzer and the determination of the heat conduction was made by heat-flow method (ASTM E1225-04) [20]. The method of immersing the specimen under water was utilized for identifying the water-absorbing ability (ASTM D570). Microstructural features of

samples were analyzed with ASONA 100X Zoom Smartphone Microscope.

### 3. RESULTS AND DISCUSSION

#### 3.1 Results

Given that the quantity of dry basic matter utilized in the manufacturing recipes was 490 g maintained constant in all tested versions, operational parameters of cellular bottle making technique are shown in Table 3.

**Table 3.** Operational parameters of the expanding procedure

Parameter	Recipe			
	R1	R2	R3	R4
Dry basic matter/cellular bottle quantity (g)	490/ 479	490/ 480	490/ 478	490/ 480
Sintering temperature (°C)	818	823	829	837
Process duration (min)	28	29	32	35
Heating rate (°C/min)	28.5	27.7	25.3	23.3
Cooling rate (°C/min)	6.9	6.7	7.1	7.0
Energy consumption (kWh/kg)	0.61	0.63	0.70	0.76

Concording with the data in Table 3, the preponderantly direct wave warming process allowed the utilize of warming rates within the limits of 23.3-28.5 °C/min, significant higher by comparison with the usual conventional procedures. Warming time was thus shortened to 28-35 min and by default, the electricity consumption of the procedure reached extremely reduced limits (0.61-0.76 kWh/kg) and was economically advantageous. The cooling of the foamed material was achieved relatively quickly, considering that the thermal inertia of the microwave oven is low. The cooling rate values (6.7-7.1 °C/min) still remained at a normal level, without creating internal stresses causing structural cracks.

Using the investigation methods mentioned in subsection 2.3, the physical, mechanical, heat, and morphological features of cellular bottle specimens were identified. The outcomes are presented in Table 4.

**Table 4.** Characteristics of cellular glass specimens

Characteristic	Recipe			
	R1	R2	R3	R4
Denseness ( $\text{g}\cdot\text{cm}^{-3}$ )	0.66	0.59	0.54	0.50
Porousness (%)	68.6	71.9	74.3	76.2
Heat conduction ( $\text{W}\cdot\text{m}^{-1}\cdot\text{K}^{-1}$ )	0.130	0.097	0.090	0.083
Compression resistance (MPa)	7.0	6.6	5.9	4.0
Water-absorbing (vol. %)	0.8	1.0	1.0	1.2
Pore size (mm)	0.1-0.2	0.1-0.4	0.3-0.6	0.3-1.0

The data in Table 4 practically show the influence of the  $\text{MnO}_2/\text{Si}_3\text{N}_4$  ratio on the characteristics of cellular glass specimens. The values of these characteristics are relatively close, because authors considered the own previous results of the reference paper [13], according to which a high ratio between the two additives negatively influences the microstructural homogeneity of the product as well as its mechanical strength. Under the conditions where between recipes R1 and R4 there is low difference between values of the mentioned ratio (from 0.89 to 1.45), the denseness decreased from 0.66 to 0.50  $\text{g}\cdot\text{cm}^{-3}$ , the porousness increased between 68.6-76.2 %, and the heat conduction decreased from 0.130 to 0.083  $\text{W}\cdot\text{m}^{-1}\cdot\text{K}^{-1}$ . At the same time, compression resistance values decreased from 7.0 to 4.0 MPa. The separate analysis of each recipe characteristics indicates that all of them are suitable for construction applications. In other words, a compensation can be observed between qualities of materials with very good heat-insulating features (R3, R4) and those with excellent compression resistance (R1, R2). In fact, the denseness of cellular bottle in the range of 0.50-0.66  $\text{g}\cdot\text{cm}^{-3}$  is considered adequate for an insulating matter as well as the compression resistance within the limits of 5.9-7.0 MPa is remarkable for this porous matter type.

Images of cellular bottle specimens are presented in Figure 2 and microstructural appearance of these specimens are shown in Figure 3.

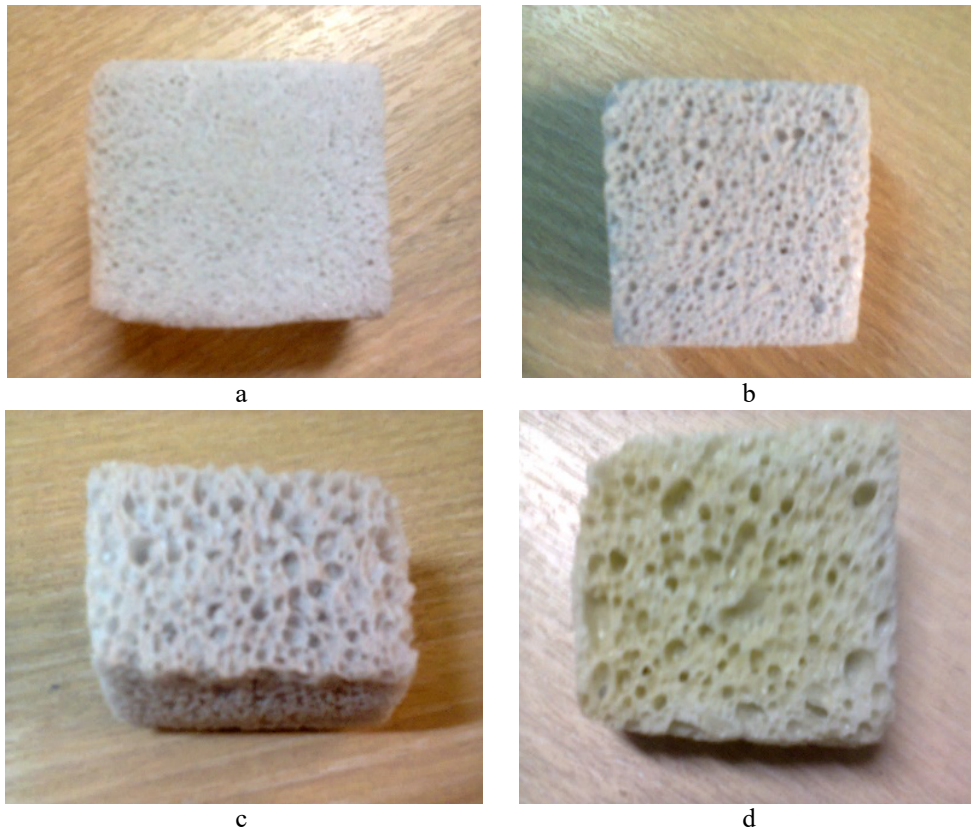


**Figure 2.** Images of cellular bottle samples  
a – recipe 1; b – recipe 2; c – recipe 3; d- recipe 4.

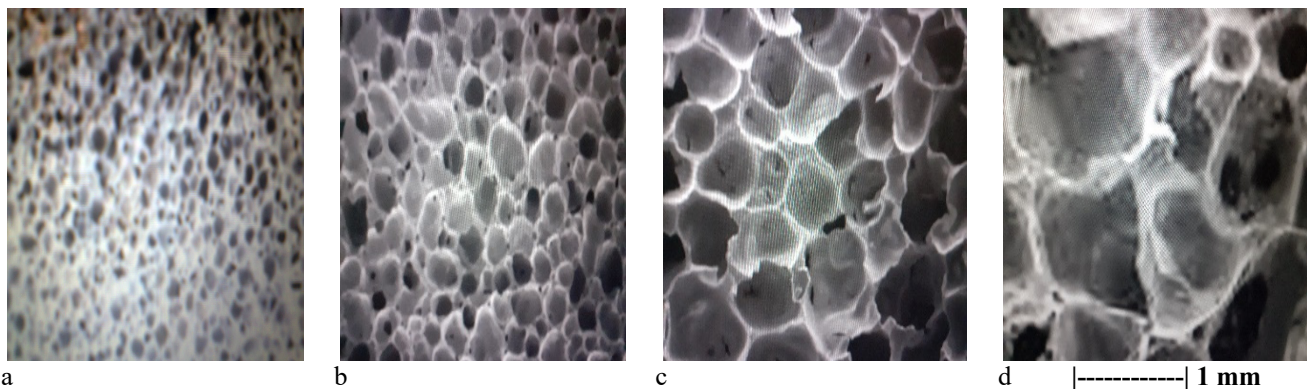


**Figure 3.** Microstructural appearance of cellular bottle specimens  
a – recipe 1; b – recipe 2; c – recipe 3; d – recipe 4.

According to Figure 2, the evolution of the specimen macrostructures from R1 to R4 can be seen. The macrostructural fineness of R1 is obvious, while the formation of R4-coarse macrostructure is easily seen.

Figure 3 shows the same evolution of the aspect of specimens, but at the microstructural scale. The pore size is increasing, its values being indicated in Table 4. Recipe R1 allowed obtaining very low sizes (0.1-0.2 mm), while recipes R2 and R3 registered slight increases (0.1-0.4 mm and 0.3-0.6 mm, respectively). R4 shows a microstructure including pores with larger sizes (0.3-1.0 mm), but also the tendency of

communication between neighbouring pores (pore coalescence).

### 3.2 Discussion

As stated above, the value variation of the  $MnO_2/Si_3N_4$  ratio could be determinant in changing the characteristics of cellular glass specimens.  $Si_3N_4$  represents the pore-supplying agent in the glass-based mixture. It is activated by creating oxidation conditions at temperatures in the range of 800-850 °C to release  $NO_2$  as gaseous bubbles. Although the reaction takes place in the oxidizing atmosphere of the furnace, it is obvious that an additional oxygen

amount is required. The oxygen-supplying agent in the case of the current experiment was chosen  $\text{MnO}_2$ , which releases gaseous oxygen through successive decomposition reactions into  $\text{Mn}_2\text{O}_3$  and  $\text{Mn}_3\text{O}_4$ . The ratio between the oxygen-supplying agent ( $\text{MnO}_2$ ) and the pore-supplying agent ( $\text{Si}_3\text{N}_4$ ) was varied through the four manufacturing recipes (R1-R4) from 0.89 to 1.45. The maximum value of this ratio was much lower compared to that used (2.75) in the reference paper [13], in order to avoid the formation of a coarse microstructure with pore coalescence, disfavoring the mechanical strength of the expanded material.

The choice of the best making recipe was influenced both by the physical, mechanical, and thermal features of cellular bottle specimens and by their microstructural homogeneity. Due to this consideration, the product manufactured using recipe R4 was excluded due to its relatively coarse microstructure.

Although it obtained the best outcome of compression resistance (7.0 MPa), the specimen corresponding to recipe R1 had significantly higher heat conduction ( $0.130 \text{ W}\cdot\text{m}^{-1}\cdot\text{K}^{-1}$ ) compared to the other specimens and the highest denseness value ( $0.60 \text{ g}\cdot\text{cm}^{-3}$ ), slightly worsening the heat-insulating properties of the specimen.

Among the specimens (b) and (c) in Figure 3, the specimen (b) manufactured with the R2 recipe was preferred, because in the microstructure of the specimen (c) several cases of coalescence of pores were observed, slightly worsening the heat-insulating properties of specimens.

According to Table 2, weight proportions of  $\text{Si}_3\text{N}_4$  and  $\text{MnO}_2$  corresponding to the manufacturing recipe R2 were equal (1.9 wt. %), their ratio being 1.0. The water added amount used as a binder was 13.5 wt. % and the residual bottle amount (post-consumer drinking bottle) was very high (96.2 wt. %).

#### 4. CONCLUSION

The work objective was the testing production of cellular bottle non-conventionally prepared from post-consumer drinking bottle having incorporated low amounts of  $\text{Si}_3\text{N}_4$  and  $\text{MnO}_2$  as a pore-forming agent and an oxygen-supplying agent, respectively. During the experiment, four making recipes (R1-R4) were tested, differing by the weight ratio of the two additives (between 0.89-1.45). Due to the remarkable energy effectiveness of the own preponderantly direct electromagnetic wave warming technique by placing a high microwave susceptible-ceramic tube, the

sintering process was short (28-35 min), the warming rates being very high ( $23.3\text{-}28.5 \text{ }^\circ\text{C}/\text{min}$ ). Also, the electricity consumption was extremely reduced (in the range of 0.61-0.76 kWh/kg). The cellular bottle specimens obtained through this process were relatively close in terms of physical, mechanical, thermal, and morphological features. Denseness within the limits of  $0.50\text{-}0.66 \text{ g}\cdot\text{cm}^{-3}$ , porousness in the range of 68.6-76.2 %, heat conduction in the range of  $0.083\text{-}0.130 \text{ W}\cdot\text{m}^{-1}\cdot\text{K}^{-1}$ , and compression resistance between 4.0-7.0 MPa characterized the four cellular bottle specimens, indicating good heat-insulating properties in correlation with excellent compression resistance. The best specimen of cellular bottle made from 96.2 wt. % recycled residual bottle, 1.9 wt. %  $\text{Si}_3\text{N}_4$ , 1.9 wt. %  $\text{MnO}_2$ , and 13.5 wt. % water addition through non-conventional warming at  $823 \text{ }^\circ\text{C}$  led to obtaining a porous product with the following characteristics: denseness of  $0.59 \text{ g}\cdot\text{cm}^{-3}$ , porousness of 71.9 %, heat conduction of  $0.097 \text{ W}\cdot\text{m}^{-1}\cdot\text{K}^{-1}$ , compression resistance of 6.6 MPa, water-absorbing of 1 vol. %, and pore size between 0.1-0.4 mm.

#### 5. REFERENCES

1. König, J., Petersen, R.R., Yue, Y., Influence of glass-calcium carbonate mixture's characteristics on the foaming process and the properties of the foam glass, *Journal of the European Ceramic Society*, Vol. 34, No. 6, pp. 1591-1598, (2014).
2. Niu, Y.H., Fan, X.Y., Ren, D., Wang, W., Li, Y., Yang, Z., Cui, L., Effect of  $\text{Na}_2\text{CO}_3$  content on thermal properties of foam-glass ceramics prepared from smelting slag, *Materials Chemistry and Physics*, Elsevier, Vol. 256, (2020). <https://doi.org/10.1016/j.matchemphys.2020.123610>
3. Goltsman, B.M., Yatsenko, A. Role of carbon phase in the formation of foam glass porous structure, *Materials (Basel)*, Pavlikova, M. (ed.), Vol. 15, No. 22, (2022). <https://doi.org/10.3390/ma15227913>
4. Paunescu, L., Axinte, S.M., Cosmulescu, F., Experimental manufacture of the foam glass gravel from glass waste and silicon carbide on a 10 kW-microwave oven, *Journal of Engineering Studies and Research*, Vol. 28, No. 3, pp. 75-81, (2022).
5. Lladis, A., Orts, M.J., Garcia-Ten, J., Bernardo, E., Foaming of flat glass cullet using  $\text{Si}_3\text{N}_4$  and  $\text{MnO}_2$  powders, *Ceramics International*, Vol. 35, No. 5, pp. 1953-1959, (2009).
6. El-Amir, A.A.M., Attia, M.A.A., Fend, T., Ewais, E.M.M., Production of high-quality glass foam

- from soda lime glass waste using SiC-AlN foaming agent, *Journal of Korean Ceramic Society*, Vol. 59, pp. 444-452, (2022).
7. Karandashova, N.S., Goltsman, B.M., Yatsenko, E.A., Analysis on influence of foaming mixture components on structure and properties of foam glass, *IOP Conf. Series: Materials Science and Engineering*, IOP Publishing, Vol. 262, (2017). <https://doi.org/10.1088/1757-899X/262/1/012020>
  8. Fernandes, H.R., Ferreira, D.D., Andreola, F., Lancellotti, I., Barbieri, L., Ferreira, J., Environmental friendly management of CRT glass by foaming with egg shells, calcite or dolomite, *Ceramics International*, Vol. 40, No. 8, pp. 13371-13379, (2014).
  9. Paunescu, L., Axinte, S.M., Dragoescu, M.F., Cosmulescu, F., Manufacture of cellular glass using oak leaves as a foaming vegetable agent, *Journal La Multiapp*, Vol. 1, No. 4, pp. 18-27, (2020). <https://doi.org/10.37899/journallamultiapp.v1i4.210>
  10. Donato, R.K., Mija, A., Keratin association with synthetic, biosynthetic and natural polymers: An extensive review, *Polymers (Basel)*, Vol. 12, No. 1, (2020). <https://doi.org/10.3390/polym12010032>
  11. Scarinci, G., Brusatin, G., Bernardo, E., Glass Foams, in *Cellular Ceramics: Structure, Manufacturing, Properties and Applications*, Scheffler, M., Colombo, P. (eds.), Wiley-VCH Verlag GmbH & Co KGaA, Weinheim, Germany, pp. 158-176, (2005). ISBN 978-3-527-31320-4. <https://doi.org/10.1002/3527606696>
  12. Garcia Ten, J., Saburit, A., Orts, M.J., Bernardo, E., Colombo, P., Glass foams from oxidation/reduction reactions using SiC, Si<sub>3</sub>N<sub>4</sub> and AlN powders, *Glass Technology-European Journal of Glass Science and Technology Part A*, Society of Glass Technology Publisher, Sheffield, UK, Vol. 52, No. 4, pp. 103-110, (2011).
  13. Dragoescu, M.F., Paunescu, L., Axinte, S.M., Glass foam made with silicon nitride and manganese oxide by microwave irradiation, *Journal La Multiapp*, Vol. 2, No. 2, pp. 1-9, (2021). <https://doi.org/10.37899/journallamultiapp.v2i2.325>
  14. Axinte, S.M., Paunescu, L., Dragoescu, M.F., Sebe, A.C., Manufacture of glass foam by predominantly direct microwave heating of recycled glass waste, *Transactions on Networks and Communications*, Vol. 7, No. 4, pp. 37-45, (2019). <https://doi.org/10.14738/tnc.74.7214>
  15. Kitchen, H.J., Vallance, S.R., Kennedy, J.L., Tapia-Ruiz, N., Carassiti, L., Modern microwave methods in solid-state inorganic materials chemistry: From fundamentals to manufacturing, *Chemical Reviews*, Vol. 114, No. 2, pp. 1170-1206, (2014). <https://doi.org/10.1021/cr4002353>
  16. Jones, D.A., Lelyveld, T.P., Mavrofidis, S.D., Kingman, S.W., Miles, N.J., Microwave heating applications in environmental engineering. A review, *Resources, Conservation and Recycling*, Vol. 34, No. 2, pp. 75-90. (2002). [https://doi.org/10.1016/S0921-3449\(01\)00088-X](https://doi.org/10.1016/S0921-3449(01)00088-X)
  17. Terayama, K., Ikeda, M., Study on thermal decomposition of MnO<sub>2</sub> and Mn<sub>2</sub>O<sub>3</sub> by thermal analysis, *Transactions of the Japan Institute of Metals*, Vol. 24, No. 11, pp. 754-758, (1983).
  18. Deschaux-Beaume, F., Cutard, T., Fréty, N., Levailant, C., Oxidation of a silicon nitride-titanium nitride composite: Microstructural investigations and phenomenological modelling, *Journal of the American Ceramic Society*, Vol. 85, No. 7, pp. 1860-1866, (2002).
  19. *Density and porosity measurements of solid materials*, Anderson Materials Evaluation, Inc. <https://andersonmaterials.com/density-and-porosity-measurements-of-solid-materials/>
  20. Yüksel, N., The review of some commonly used methods and techniques to measure the thermal conductivity of insulation materials, in *Insulation Materials in Context of Sustainability*, Almusaed, A., Almsaad, A. (eds.), ISBN 978-953-51-2625-6, (2016). <https://doi.org/10.5772/64157>